Applied Energy 374 (2024) 124042

Contents lists available at ScienceDirect

Applied Energy

journal homepage: www.elsevier.com/locate/apenergy

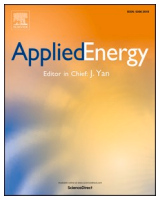

Dissociation behavior of sI and sII gas hydrates in response to environmental changes – Investigations on the self-preservation effect

Parisa Naeiji [a,b,**], Manja Luzi-Helbing [a], Judith M. Schicks [a,*], Mengdi Pan [a,b]

[a] GFZ German Research Centre for Geosciences, Telegrafenberg, 14473 Potsdam, Germany
[b] School of Chemical and Bioprocess Engineering, University College Dublin, Belfield, Dublin, Ireland

HIGHLIGHTS

- Dissociation behavior of sI and sII gas hydrates was studied at subzero temperatures and pressures > 0.1 MPa.
- While the sI hydrates exhibited delayed decomposition, the sII hydrates decomposed continuously.
- Hydrate reformation prevents the continuous decomposition of sI hydrates.
- The gas hydrates composition impacts their dissociation behavior, as the released gas molecules affect each other.

GRAPHICAL ABSTRACT

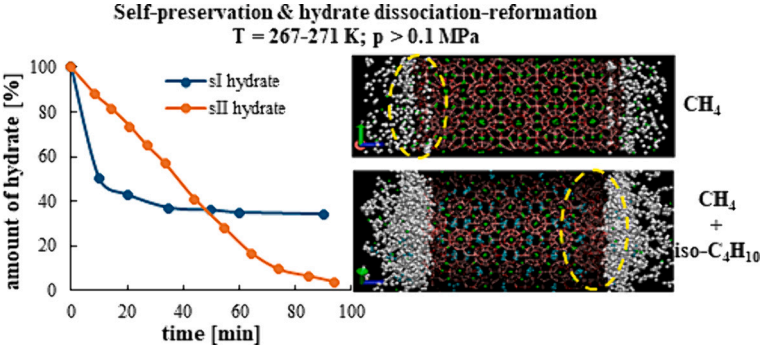

ARTICLE INFO

Keywords:
Gas hydrate
Dissociation
Self-preservation
Environmental change
Molecular dynamics simulation
Powder X-ray diffraction measurements

ABSTRACT

Natural gas hydrates are ice-like solids occurring worldwide on continental margins and in permafrost regions. Their high methane (CH_4) content makes them a potential energy source, but also a climate factor. Pressure and temperature changes in their environment may induce the decomposition of gas hydrates. Some hydrates, however, exhibit a so-called self-preservation effect which delays the decomposition process and is not yet sufficiently understood. In the present work, the decomposition behavior of simple and mixed sI and sII hydrates was studied via experiments ($T = 267–271$ K; $p > 0.1$ MPa) and numerical modeling. This combined approach led to new insights into which molecule-specific properties result in a self-preservation effect. The results show that CH_4 and especially CO_2 intend to participate in hydrate reformation whereas hydrates including heavier hydrocarbon molecules do not undergo a decomposition–reformation process, and thus these hydrates continued dissociating with no barrier. Under certain conditions, a liquid C_4-hydrocarbons phase is preferentially formed in which C_4-hydrocarbons are enriched. Generally, the dissociation rate seems to depend on the composition of the hydrates, and the behavior of CH_4 molecules in the dissociation process is influenced by the presence of other gases in the mixed gas hydrate.

* Corresponding author at: GFZ German Research Centre for Geosciences, Telegrafenberg, 14473 Potsdam, Germany
** Corresponding author at: School of Chemical and Bioprocess Engineering, University College Dublin, Belfield, Dublin, Ireland
E-mail addresses: parisa.naeiji@ucd.ie (P. Naeiji), schick@gfz-potsdam.de (J.M. Schicks).

https://doi.org/10.1016/j.apenergy.2024.124042
Received 21 February 2024; Received in revised form 18 July 2024; Accepted 24 July 2024
Available online 3 August 2024

1. Introduction

Natural gas hydrates are composed of water and gas molecules, with the water molecules forming defined cavity structures via hydrogen bonds, which are stabilized by the inclusion of gas molecules. Depending on the size of the guest molecules, different types of cavities are formed. Natural gas hydrate reservoirs are supposed to store a high density of CH_4 and other hydrocarbons which led to the formation of three types of hydrate structures: structure I (sI), structure II (sII), and structure H (sH) [1,2]. They form at low temperatures and elevated pressures and could be detected in permafrost regions or marine environments [1,3]. They are susceptible to the key perturbations associated with environmental changes, namely decreases of pressure and increases in ocean/permafrost temperatures [4,5]. The decomposition of gas hydrates by widespread destabilization of deposits trapped in marine and permafrost-associated sediments could liberate large volumes of climate-influencing gas [6–9].

Some kinds of gas hydrates can prevent themselves from further decomposition below the melting point of water and remain as a metastable hydrate phase at pressure and temperature conditions outside the hydrate stability region [5]. This metastability is thought to be caused by a layer of ice formed at the surface of the hydrate particle when the gas hydrate decomposes, and this ice layer coats the hydrate surface to protect it from further decomposition [10–12]. This behavior has been called “anomalous self-preservation” [13–15] and can have implications for natural gas storage [16].

A series of macroscopic and microscopic investigations of hydrate dissociation kinetics upon self-preservation have been performed so far [5,13,17–20]. Most of them have studied this mechanisms under atmospheric pressure (0.1 MPa) and temperatures lower than 273.15 K. Stern et al. observed two temperature regimes (245–255 K and 265–271 K at 0.1 MPa) showing a pronounced self-preservation effect for simple CH_4 hydrate [13]. At temperatures around 268.15 K, simple CH_4 hydrate exhibits metastability for several days at atmospheric pressure [13,17,19]. With the hypothesis that a defective, stacking-faulty ice layer initially forms around hydrate particles at temperatures below 240 K, which transforms into a dense and closed ice Ih mantle at temperatures above 240 K, Kuhs et al. provided a first explanatory approach for the self-preservation effect [12]. This approach, however, could not explain why the self-preservation effect was not observed for other hydrates which, for example, contained C_3H_8 or a mixture of CH_4 and C_2H_6. Takeya and Ripmeester studied the dissociation behavior of different gas hydrates, including sI hydrates (CH_4, CH_3F, CF_4, and CO_2 hydrates) and sII hydrates (O_2, N_2, Ar, and Kr hydrates), between 153 K and 273 K at 0.1 MPa. They found that self-preservation depends on the interaction strength between guest and ice and that hydrates with higher dissociation pressures tend to show self-preservation phenomena. In addition, the guest molecules may be trapped in the newly formed ice phase and thus support the formation of amorphous ice during the hydrate dissociation [20]. In another study Takeya et al. described the two-regime CH_4 hydrate dissociation process: the first step was the formation of an ice layer around the CH_4 hydrate, and in the second step the CH_4 had to diffuse through the thickening ice layer so that the second step determined the hydrate lifetime [18]. Higher hydrocarbons like C_2H_6 and C_3H_8 hydrates were considered to show no preservation phenomenon, and a mixture of them with CH_4 reduces the preservation ability of CH_4 hydrate [14,19,21]. Zhong et al. confirmed that self-preservation is selective; CH_4 shows a stronger self-preservation effect than C_2H_6. The selective self-preservation effect of CH_4 over C_2H_6 results in the structural transition and this selectivity increases with decreasing the temperature [19].

From the literature cited above, the anomalous preservation of the gas hydrate phase is presumably attributed to the formation of the ice layer on the hydrate crystals that results in a decrease in the further diffusion of the guest molecules, however, the molecular mechanism of the self-preservation phenomena that causes this effect, remains unclear. Due to the temporal and spatial limitations of the monitoring techniques, the molecular simulations could be a potential way to provide microscopic insights into gas hydrate dissociation. Several molecular dynamics (MD) simulations were performed to clarify the self-preservation effect on the gas hydrate dissociation [22–24]. By MD simulations, Tse and Klug found that the released water molecules reassemble into a solid-like structure next to the hydrate surface to block its further dissociation [15]. There is a coupling between the heat transfer resistance and the mass transfer resistance as the driving mechanism for the self-preservation effect that is enhanced by increasing the pressure and especially decreasing the temperature [25].

The dissociation process of gas hydrates has mostly been studied at atmospheric pressure (0.1 MPa) and below the freezing point of ice. But little is known about the dissociation behavior at pressures below the equilibrium pressures at given temperatures but higher than 0.1 MPa, which might be a more realistic condition for hydrate dissociation in nature. Therefore, the knowledge of the dissociation behavior under these specific conditions and the occurrence of metastable gas hydrate phases due to the self-preservation effect is a critical issue. Experimental work by Chuvilin et al. showed that the gas hydrates in permafrost are stable from a depth of about 250 m, however, they could also be found in shallower permafrost layers from a depth of 150–200 m above at temperature and pressure conditions out of their thermodynamic stability, which is called a zone of metastable hydrates [5,26]. The metastable gas hydrates are supposed to exist for quite long periods of time in permafrost above the hydrate stability zone, nevertheless, it should be recognized that these occurrences are particularly vulnerable to pressure and temperature changes in their environment [10]. Most of the gas hydrate deposits associated with permafrost are on the edge of gas hydrate stability, which could become a problem if global warming causes both the gas hydrates to decompose and the permafrost to thaw, releasing harmful greenhouse gases [4,27]. Even though, this self-preservation effect has also several potential advantages in engineering applications, such as gas storage and transportation [16].

Our experimental study extends the existing ideas on the mechanisms of gas hydrate self-preservation in permafrost in which gas hydrates may contain C_1-C_4 hydrocarbons as well as carbon dioxide at pressures higher than 0.1 MPa and temperatures between 267 K and 271 K to simulate conditions in a natural environment. Literature showed that the self-preservation effect depends on the guest molecules in addition to the temperature and pressure conditions [14,19–21]. It is therefore worth studying how the guest molecules affect the self-preservation effect at these pressure and temperature conditions. For providing a better estimation, we also used numerical modeling to understand the molecular interactions.

2. Methods

2.1. Experimental

Time-resolved powder X-ray diffraction (PXRD) measurements were done using a low-temperature-high-pressure cell integrated into a Brucker AXS D8 Discover micro-diffractometer. The cell can be operated in a temperature range of 253–288 K and a pressure of 0.1–4.0 MPa. It is running with a continuous gas flow of about 1 ml/min ensuring a constant composition of the gas phase during the whole experiment. The diffractometer has parallel beam optics (Goebel mirror) to optimize the beam intensity, enabling the analysis of powder samples with a non-planar surface. A mono-capillary reducing the beam diameter to 300 μm was applied. Due to the narrow beam, several positions within the sample can be measured in a short sequence, which enables a better statistical interpretation. The detection of the diffracted X-rays is done via GADDS (General Area Detection Diffraction System) including a HI-Star area detector. More detailed information can be found by Luzi et al. [28].

In preparation of a time-dependent experiment, the precooled

sample cell was filled with approximately 150 µl powdered ice, carefully sealed and mounted on the XYZ stage of the diffractometer. The ice used for the experiments was prepared from ca. 3 ml deionized water, which was frozen in a liquid nitrogen bath, and then powdered in a 6750 freezer mill (Spex CertiPrep) to a diameter of <10 µm. After the ice was filled into the pressure cell, it was pressurized with the respective gas or gas mixture. After the complete conversion of ice into hydrate, which was proven by powder X-ray diffraction measurements, the pressure was decreased to 50% below the equilibrium pressure at 271 K for the sI hydrates and 267 K for the sII hydrates, respectively. The equilibrium conditions were calculated for the hydrates formed from the respective gas mixtures using CSMGem, as shown in Fig. 1. A list of the gas systems used in this study as well as the p-T conditions for dissociation experiments are given in Table 1 as well as in Fig. 1. The dissociation process was monitored by continuously recording the powder X-ray pattern of the hydrate samples.

2.2. Molecular dynamics simulation

For doing the molecular dynamics simulations, the GROMACS program (version 2021) was used [29]. The dissociation process of the gas hydrates was studied using two different configurations: (1) 3 × 3 × 6 unit cell replica of sI hydrate with a dimension of 3.64 nm × 3.64 nm × 7.11 nm, and (2) 2 × 2 × 4 unit cell replica of sII hydrate with a dimension of 3.54 nm × 3.54 nm × 7.11 nm. The hydrate phase was placed in the center of a simulation box with a vacuum on each side of the hydrate in the *z*-direction to provide free interfaces where heterogeneous decomposition began. The periodic boundary conditions were used in all directions.

The initial coordinates of the atoms of the water molecules in the unit cells are from the work of Takeuchi et al. [30]. All hydrate cavities of sI hydrate were occupied by gas molecules. The initial gas compositions and cavity occupancy for the mixed gas hydrates, as given in Table 2, were approximated as the equilibrium compositions of the hydrate phases calculated with CSMGem software [1]. The feed gas was considered based on the information presented in Table 1. In the case of sII hydrates, two more hydrate compositions with lower cavity occupation than that of CSMGem calculations were also studied to see the effect of hydrate cavity occupancy on the dissociation process, which is discussed later in the result section.

The TIP4P/Ice model was used for modeling the intermolecular

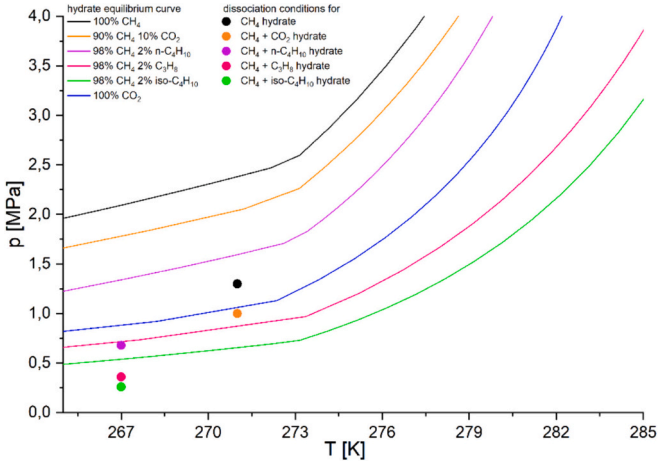

Fig. 1. p-T-equilibrium curves calculated with CSMGem [1] as well as the experimental dissociation conditions for the gas hydrate phases formed from the respective feed gas. Depending on the size and shape of the encased gas molecule, the occupied cavity will be ideally filled (e.g. isoC_4H_{10}) or – if the molecule is slightly too large – distorted (e.g. n-C_4H_{10}), which has a direct impact on the stability range of the respective hydrate phase.

Table 1
The gas systems and the p-T conditions for dissociation experiments in this work.

Gas system	Temperature (K)	Pressure (MPa)
100% CH_4	271	1.30
10% CO_2 + 90% CH_4	271	1.00
2% C_3H_8 + 98% CH_4	267	0.36
2% n-C_4H_{10} + 98% CH_4	267	0.68
2% isoC_4H_{10} + 98% CH_4	267	0.26

interactions of water molecules [31], while CO_2 and hydrocarbon molecules were modeled by TraPPE [32] and TraPPE united atom [33] potentials, respectively. All internal structures of the molecules were kept rigid by using the LINCS algorithm [34]. In addition, the Lorentz-Berthelot combining rules was used to determine the cross-interaction parameters between atoms on different molecules [35]. The Particle Mesh Ewald method [36,37] was also applied to evaluate the electrostatic interactions as the sum of the van der Waals and long-range Coulomb potentials with a relative error of 10^{-6} and an overall cutoff of 1.4 nm.

The temperature and pressure of the simulation were kept constant using Nose-Hoover thermostat [38] and the Parrinello-Rahman barostat [39], respectively, by the *NPT* ensemble. The equations of motion were integrated using the Leap-frog algorithm [40] at each time step of 2 fs. The hydrate dissociation conditions implemented in the simulations were identical to the experimental conditions for the PXRD measurements, as given in Table 1.

3. Results and discussion

3.1. Powder X-ray diffraction measurements

Gas hydrates were formed from ice and the respective gas mixture within the pressure cell (see Methods). In order to monitor the hydrate dissociation process, the pressure was chosen 50% below the calculated equilibrium pressure of the respective gas hydrates at 271 K for the sI hydrates and 267 K for the sII hydrates. The hydrate dissociation process was monitored by recording continuously powder X-ray diffraction (PXRD) pattern at five different spots on the sample surface. Fig. 2(a) shows the results obtained from the PXRD measurements during the dissociation of simple CH_4 hydrates and mixed CH_4+CO_2 hydrates, which are both sI hydrates. Fig. 2(b) shows the results obtained during the dissociation of sII mixed hydrates, containing C_3H_8, n-C_4H_{10} and iso-C_4H_{10} besides CH_4. The results indicated a fast dissociation process within the first 5–10 min. Thereafter, the dissociation rate for the sI hydrates decreased significantly and appears to stagnate at a hydrate content of 35% ± 5% (CH_4) and even 60% ± 5% (CH_4+CO_2). This behavior suggests the occurrence of the frequently-described self-preservation effect. Such a behavior was not observed for the mixed sII hydrates as represented in Fig. 2(b). The mixed sII hydrates were completely dissociated within a certain time, however, they showed different dissociation rates among each other. The results clearly showed that the sII hydrate including n-C_4H_{10} were already completely dissociated after 20 min. The mixed CH_4+C_3H_8 and CH_4+iso-C_4H_{10} showed no hydrate signals after ca. 80 and 120 min, respectively.

In summary, the simple and mixed sI hydrates showed a self-preservation effect, but the mixed sII hydrates did not. On closer examination, all hydrates showed individual decomposition behavior depending on their composition. In the case of the CH_4+CO_2 mixed sI hydrate, the self-preservation effect seemed to be more pronounced than in the case of the pure CH_4 hydrate due to the presence of CO_2. In the case of the mixed sII hydrates, the dissociation rate highly depended on the properties of the larger hydrocarbon molecule. This might be related to the ability of the large guest molecules to stabilize the $5^{12}6^4$ cavities. It should be noted that in the case of mixed CH_4+n-C_4H_{10} hydrate, the n-C_4H_{10} molecule is incorporated into the $5^{12}6^4$ cavity as its gauche

Table 2
Gas compositions and cavity occupation in the mixed hydrate phases used in this work.

Gas system	Gas component	Feed gas (%)	Fractional cavity occupancy - CSMGem			Number of gas molecules in the unit cell - This work								
			S[a]	L[b]	%[c]	S[a]	L[b]	%[c]	S[a]	L[b]	%[c]	S[a]	L[b]	%[c]
$CH_4 + CO_2$	CH_4	90	0.7918	0.7374	81.63	2	5	87.5						
	CO_2	10	0.0320	0.2147	18.37	0	1	12.5						
$CH_4 + C_3H_8$						83.3% occupied			70.8% occupied			62.5% occupied		
	CH_4	98	0.7376	0.1012	64.04	12	1	65.0	10	1	64.7	9	0	60.0
	C_3H_8	2	0.0000	0.8850	35.96	0	7	35.0	0	6	35.3	0	6	40.0
$CH_4 + n\text{-}C_4H_{10}$						91.6% occupied			83.3% occupied			70.8% occupied		
	CH_4	98	0.8407	0.4270	79.55	14	3	77.3	12	3	75.0	12	0	70.6
	$n\text{-}C_4H_{10}$	2	0.0000	0.5417	20.45	0	5	22.7	0	5	25.0	0	5	29.4
$CH_4 + isoC_4H_{10}$						87.5% occupied			70.8% occupied			62.5% occupied		
	CH_4	98	0.7808	0.1052	65.39	13	1	66.7	10	1	64.7	9	0	60.0
	$isoC_4H_{10}$	2	0.0000	0.8821	34.61	0	7	33.3	0	6	35.3	0	6	40.0

[a] S: Small cavity.
[b] L: Large cavity.
[c] %: Percentage of the gas molecule.

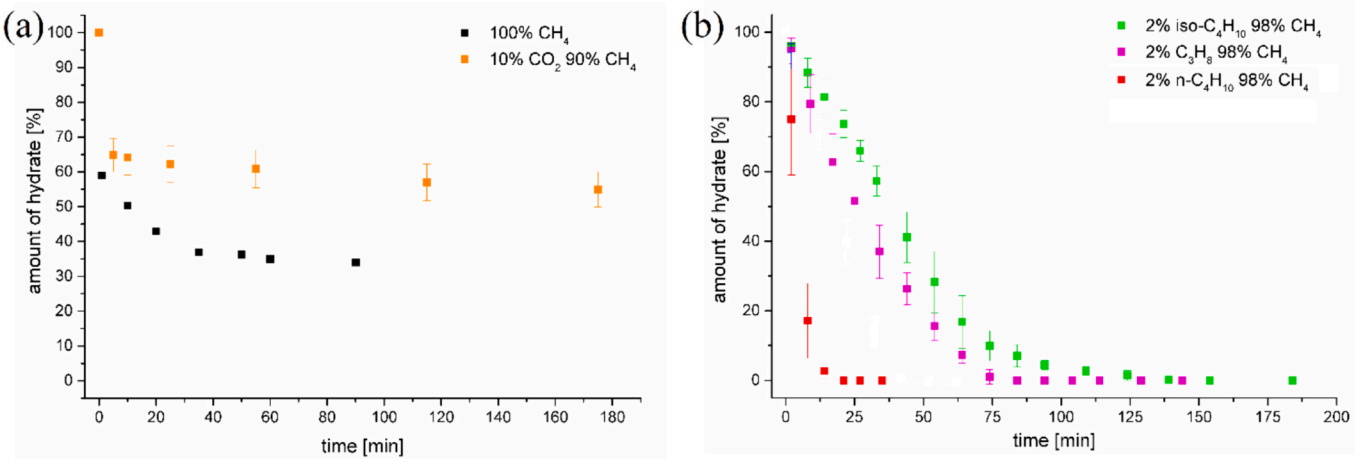

Fig. 2. Results from time-dependent in situ PXRD experiment monitoring (a) sI and (b) sII hydrates dissociation.

conformer leading to a deformation of the $5^{12}6^4$ cavities [41,42]. In contrast, the more spherical iso-C_4H_{10} molecules ideally fill the $5^{12}6^4$ cavities and thus contribute significantly to a general stabilization of the hydrate structure, which is reflected in a shift of the pressure and temperature equilibrium curve towards lower pressures and higher temperatures, respectively, as seen in Fig. 1. This is also reflected in the dissociation enthalpy of CH_4+n-C_4H_{10}, which is lower than that of both CH_4+C_3H_8 and CH_4+iso-C_4H_{10} at approximately the same composition, with CH_4+iso-C_4H_{10} exhibiting the highest value. The dissociation enthalpy is contingent upon the fit of the guest species into the hydrate cavity and the extent of its occupation [43]. This would be an explanation for the different decomposition rates in the mixed sII hydrates but would not explain why the sII hydrates do not exhibit any self-preservation effect at all. This is even more surprising since the ratio of the enclosed molecule size to the size of the hydrate cavity (guest-to-cavity ratio) has a considerable influence on the stability conditions of the respective hydrate phase. During decomposition, however, this form of cavity stabilization seems to play only a minor role, since only the less stable sI hydrates exhibit a clear self-preservation trend. To our knowledge, these observations could not be clarified so far and will be investigated in more detail in the following MD simulation part.

3.2. MD simulation of gas hydrate dissociation

The dissociation of CH_4 hydrate and binary CH_4+CO_2, CH_4+C_3H_8, CH_4+iso-C_4H_{10}, and CH_4+n-C_4H_{10} hydrates were also studied via MD simulations. From the literature, it is hypothesized that the ice layer on the hydrate crystals can cause the anomalous preservation of the gas hydrate; however, the gas hydrates may partly convert to ice and back, and ice may undergo metamorphism in a recrystallization zone at the ice-hydrate boundary [12,20]. The nucleation of hydrates is controlled not only by temperature but also by the pressure of the gas. Previous observations have indicated the gas hydrate reformation during the depressurization stage [44]. The main cause of hydrate reformation was identified to be insufficient heat supply for hydrate dissociation. Also, the pressure, which may increase locally due to the release of gas molecules during the dissociation of the gas hydrates, can induce a reformation of the gas hydrates [45]. Nevertheless, the role of gas molecules and their participation in dissociation-reformation process as a part of self-preservation has not been sufficiently studied so far. Therefore, the main goal of this study is not to prove the formation of ice, but to show how different guests can influence the self-preservation effect of gas hydrates.

To do this, several criteria were taken into account for quantitatively characterizing the dissociation process.

Simulation trajectory. For understanding what really happened during gas hydrate dissociation and why the dissociation of the simple CH_4 and the mixed CH_4+CO_2 hydrate was stopped, the simulation trajectories were provided as shown in Fig. 3. In addition, some animations of the simulations were generated as Supporting Information. All molecular visualizations in this work were provided by using the VMD software [46]. The hydrogen-bonded water molecules are displayed in red in Fig. 3. The modeling shows that the water molecules do not transform into an ordered ice structure during the hydrate dissociation

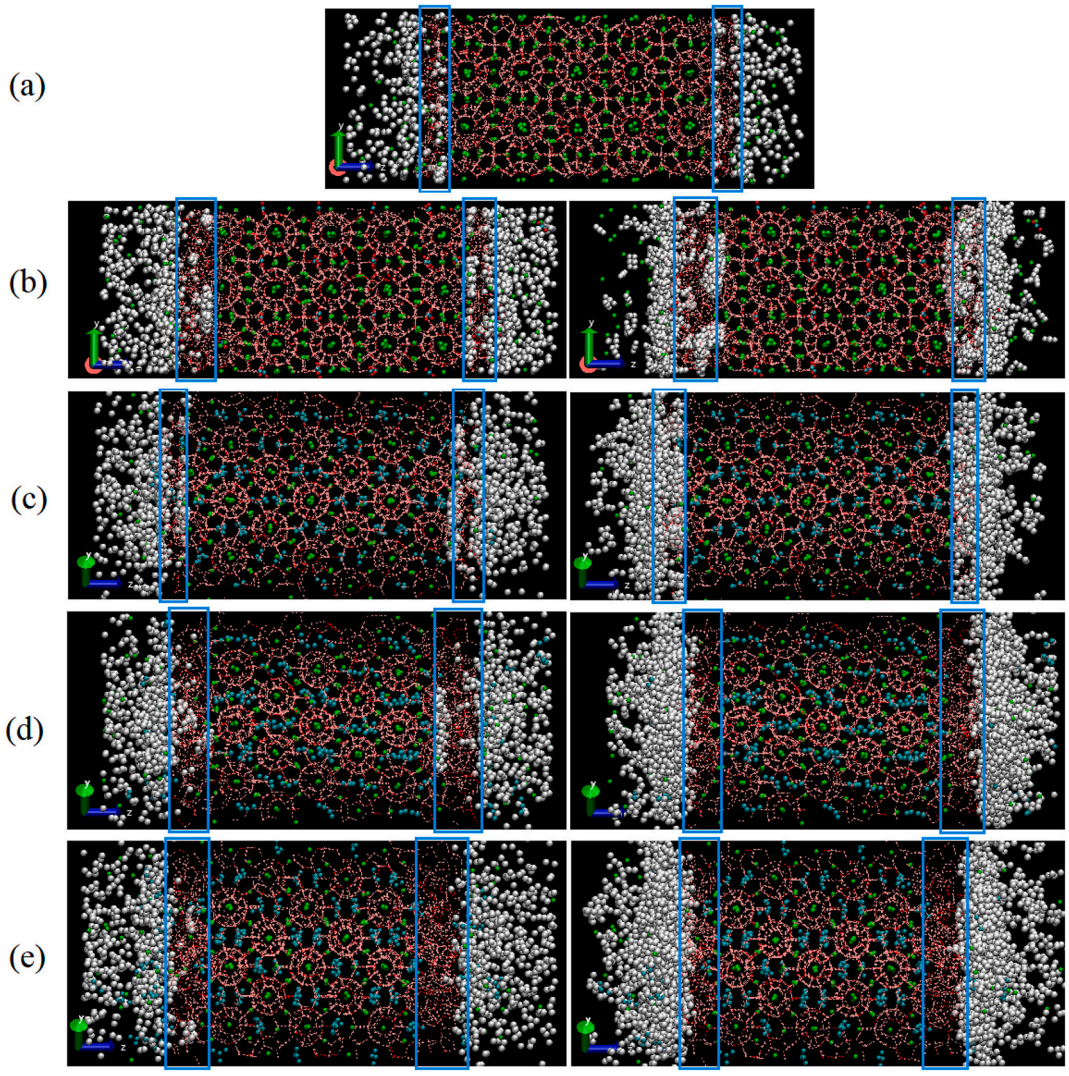

Fig. 3. Trajectories of gas molecules during the hydrate dissociation simulations for (a) CH_4 hydrate and (b) $CH_4 + CO_2$ hydrate, (c) $CH_4 + C_3H_8$ hydrate, (d) CH_4-n-C_4H_{10}, and (e) $CH_4 + isoC_4H_{10}$ hydrate. The left-hand side figures of (b)-(e) are trajectories of CH_4 molecules and the right-hand ones are for another gas molecule in the system. The hydrogen-bonded water molecules are shown by the red lines and also on the last simulation frame. CH_4 and CO_2 are shown by green and cyan-red, respectively, and other gas molecules are indicated by cyan. White spheres show the trajectories of one single gas molecule over the simulation. The quasi-liquid region is indicated by the blue rectangles. Here are snapshots of sII hydrates at their highest cavity occupancy, as detailed in Table 2. (For interpretation of the references to colour in this figure legend, the reader is referred to the web version of this article.)

process, but remain disordered, as in a liquid phase, on the hydrate surface. We refer to this as a quasi-liquid layer, which is indicated by the blue rectangles in Fig. 3. CH_4 and CO_2 are shown by green and cyan-red, respectively, and other gas molecules are indicated by cyan. The trajectories of single gas molecules (displayed as white spheres in Fig. 3) at the surface are shown over the simulation to track the molecular pathway of gas molecules during the dissociation process. In this scenario, all molecules were held stationary at the final frame of the simulation, except for one specific gas molecule chosen as a representative of its type. This molecule, situated somewhat on the surface, was influenced by the initial stages of hydrate dissociation. Therefore, these trajectories can be assigned to represent the behavior of the majority of released gas molecules during the simulation.

As seen in the figure, only the surface of the CH_4 and CH_4+CO_2 hydrate were dissociated, but some water molecules from the dissociated hydrate may be highly rearranged and recrystallized to hydrate cavities, so that no further dissociation was observed. A large proportion of the released gas molecules stay at the gas phase or adsorb on the gas/liquid surface, however, a part of these molecules intends to return to the quasi-liquid phase or even stay in this phase after hydrate dissociation for reforming the hydrate cavities. Those white spheres, which were transferred to the hydrate surface, represent the contribution of this molecule to the hydrate reformation. Thus, throughout the process, the hydrate undergoes a decomposition–reformation process and this results in the temporary slowdown or stopping of gas release. This process can affect the gas hydrate self-preservation, which depends on how much of the released gas molecules participate in the reformation process. For the sI hydrates, both CH_4 and CO_2 molecules intend to remain in the quasi-liquid phase (Fig. 3a and b). Especially CO_2 molecules show a greater tendency to do so. The right side of Fig. 3b which refers to CO_2 molecules, illustrates a larger contribution of the tracked gas molecule at the hydrate interface layer, which is likely the case for the majority of the released CO_2 molecules. If a greater number of gas molecules accumulate in the quasi-liquid phase, the reformation pressure is expected to increase, leading to a higher possibility of hydrate reformation. This could explain why the mixed CH_4+CO_2 sI hydrates showed a more pronounced self-preservation effect in the experiment than the pure CH_4 hydrate.

In the case of the mixed sII hydrates (Fig. 3c-e), the simulation showed differences compared to sI hydrates. The contribution of gas

molecules remaining in the hydrate phase and the quasi-liquid layer is not as significant as in sI hydrates. CH_4 appears to remain partially in the decomposing hydrate structure, but when it leaves the hydrate structure, it also moves away from the surface of the hydrate. The higher hydrocarbons migrate directly to the surface but remain there slightly longer, as indicated by a greater number of white spheres at the gas/quasi-liquid surface. However, for the CH_4+C_3H_8 hydrate, both CH_4 and C_3H_8 seem to remain in/revert to the quasi-liquid layer (Fig. 3c) and thus can participate somehow in the hydrate reformation. In fact, significant diffusion of gas molecules in the quasi-liquid phase temporarily hinders further dissociation. It was previously found that C_3H_8 molecules preferentially align parallel to the gas/water interface and show a stronger interaction with water molecules [47]. This results in the CH_4+C_3H_8 hydrate being more preserved over the simulation time and showing an irregular dissociation process. Such behavior could not be observed in the PXRD measurements; however, it should be noted that this effect strongly depends on the cavity occupancy and the reformation process becomes weaker by decreasing cavity occupancy. It is very likely that the experimentally formed hydrates, especially sII hydrates, are not perfect in terms of full occupancy of the cavities. They rather exhibit both partial occupancy of the cavities and defects in their structure (discussed below) in which both reduce the stability of the cavities and the hydrate structure compared to an idealized structure in the simulation. In addition, it should be considered that a continuous gas flow was used in the experiment, so that the gas molecules released from the hydrate phase were partially removed away from the surface, preventing strong interaction with the quasi-liquid phase. This aspect becomes more important in the use of heavier hydrocarbons because the re-migration of the larger hydrocarbons into the quasi-liquid layer is lower than that of sI hydrate formers (CH_4 and CO_2), which can easily accumulate in this area. In the numerical simulations, however, the CH_4+C_3H_8 hydrate behaves somehow different from the other two sII hydrates. It seems that the gas molecules of the CH_4+iso-C_4H_{10} and CH_4+n-C_4H_{10} systems (Fig. 3d and e) leave the hydrate phase, move directly to the gas phase and do not return to the quasi-liquid phase anymore. It was stated that n-C_4H_{10} cannot fit into a cavity without distortion since its size ratio of guest diameter/cavity diameter is a little higher than upper bound of about 1.0 indicating a deformation of the cavity as a result of its incorporation and thus a less significant cavity stability [41,42]. Some snapshots of single $5^{12}6^4$ cavity occupied by n-C_4H_{10} during the simulation were shown in Fig. 4, which clearly shows that the gas rotation causes distortion in the cavity. Moreover, due to the shape restriction, n-C_4H_{10} can fit into the hydrate cavity only in its gauche conformation rather than the anti-conformation in agreement with those previously stated in the literature [48]. The effect of CH_4 molecules on the reformation process is also reduced in these systems. Therefore, these hydrate structures are gradually decomposed with no self-preservation effect. Fig. 5 illustrates the density profiles of larger hydrocarbons and water in sII hydrates at 1 ns and 600 ns of the simulation, at approximately the same compositions. Over this period, a notable migration of larger molecules to the gas phase occurred, enriching the gas/quasi-liquid surface and resulting in an increase in surface density. While C_3H_8 could revert into the quasi-liquid phase, both iso-C_4H_{10} and n-C_4H_{10} did not return into the quasi-liquid phase. This observation is consistent with the water density, which exhibits a smooth curve in the region where the last-mentioned gas molecules no longer exist.

The selected experimental p-T-conditions avoid the condensation of one of the gas phases from the feed gas phase, which also flows through the cell during decomposition. This is shown by the values for the vapor pressures and dew points in Table S1. It should be noted, however, that CO_2 and the higher hydrocarbons C_3-C_4 are preferred incorporated into the hydrate phase during the formation process (see Table 2). This enrichment in the hydrate phase means that the gas mixture released during the decomposition of the hydrate also contains significantly higher proportions of CO_2, C_3H_8, iso-C_4H_{10} or n-C_4H_{10} compared to the initial feed gas phase. In the case of iso-C_4H_{10} and n-C_4H_{10}, the release of the increased proportions of these molecules may preferentially result in the formation of a liquid hydrocarbon phase and not in hydrate reformation, as the partial pressure of the components iso-C_4H_{10} or n-C_4H_{10} may become higher than the corresponding vapor pressure of these components at a given temperature. In contrast, gas mixtures containing C_3H_8 or CO_2 in addition to CH_4 do not form a liquid phase under the given p-T conditions. These gases are still available for hydrate reformation. Since CO_2 shows a significantly (20–44 times) higher solubility in water compared to hydrocarbons at temperatures $\geq$273.15 K, one can also assume a higher affinity of CO_2 for the quasi-liquid layer, so that it can easily be incorporated back into hydrate cages. This could explain why the CH_4+CO_2 mixed hydrate has a particularly pronounced self-preservation effect. However, it should also be noted that the p-T-conditions at which the decomposition of the CH_4+CO_2 mixed hydrate was studied are outside the stability limits of a pure CO_2 hydrate, as can be seen in Fig. 1. We can therefore rule out the possibility that the observed delay in the decomposition of the original mixed CH_4+CO_2 hydrate is due to the formation of a hydrate that is stable under these p-T-conditions.

Hydrate cavity number. The hydrate cavity number was also counted throughout the simulation to assess the involvement of released gas molecules in the reformation process during the dissociation. Fig. 6 plots the smoothed time variation of the cavity clusters for all hydrate systems. It should be noted that this calculation was done with the codes in Python developed by Chen et al. [49,50] and that it includes all possible cavity types of each structure. In the initial phase of the dissociation, the number of cavities suddenly decreased due to the collapse of the incompletely open cavities at the surface. Thereafter, the decrease continues more slowly or was even stopped with some fluctuations. The fluctuation or increase in the cavity number indicates a hydrate reformation during the process. The results are in agreement with those found in the previous subsections. Some hydrates can maintain a constant number of cavities during the process, even in the

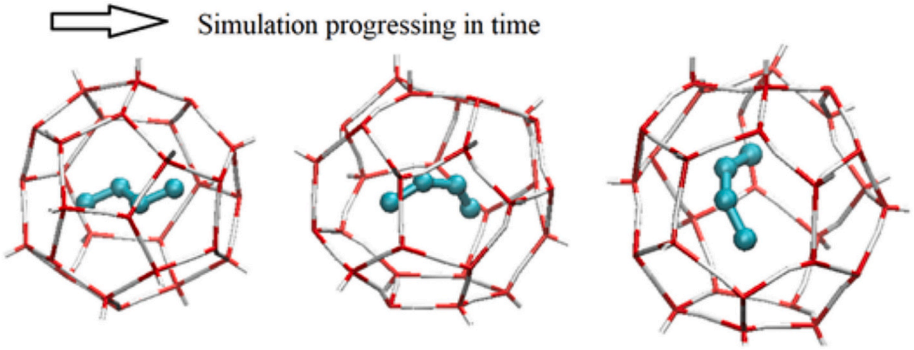

Fig. 4. The distortion of $5^{12}6^4$ cavities occupied by n-C_4H_{10} molecules during the simulation.

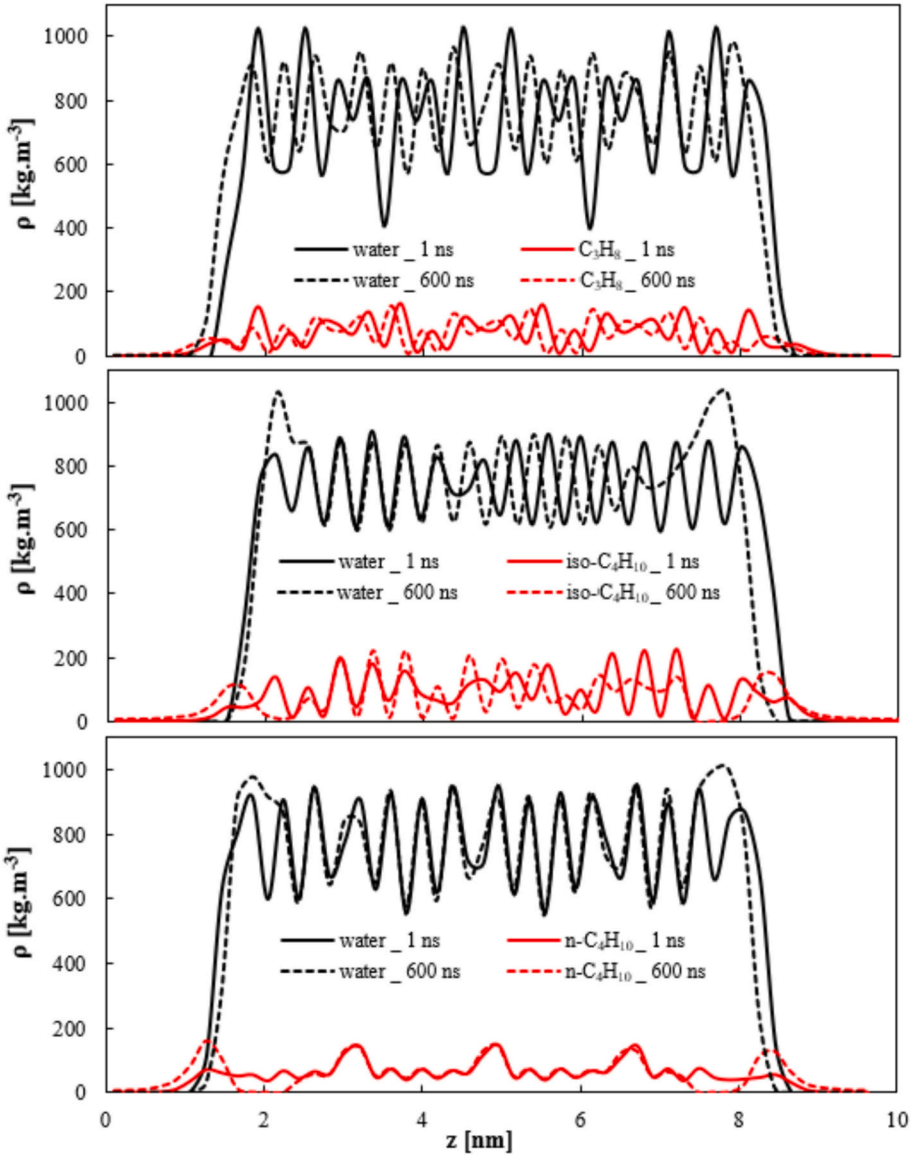

Fig. 5. The *z*-density profiles for water and (a) C_3H_8, (b) isoC_4H_{10} and (c) n-C_4H_{10} molecules of sII hydrate systems with the occupancy of 70.8% at 1 ns and 600 ns of the simulation times.

presence of significant or minor fluctuations. However, others exhibit an inability to do so, leading to a very slow progression of dissociation.

As depicted in Fig. 6a and b, following a rapid decline in the number of cavities up to approximately 20 ns, the calculations exhibited a relatively stable trend, although with more pronounced fluctuations in the case of system involving CO_2. For the sII hydrates, a different dissociation behavior was observed in the simulations, depending on the numbers of cavities occupied. By decreasing the cavity occupancy, the dissociation process gets faster, meaning that not only the surface but also the inner parts of the hydrate were involved in the dissociation. The dissociation of CH_4+C_3H_8 hydrate with 83.3% cavity occupancy showed no significant dissociation. The dissociated layers partly returned to the hydrate phase implying that the gas molecules effectively intend to be re-captured by the incomplete hydrogen-bonded water networks, however, it was not a stable situation, and the hydrate slabs may later completely be dissociated. A similar irregular manner was also observed for the two other systems involving CH_4+C_3H_8 hydrates; the dissociation progress appeared somewhat accelerated. The last two sII hydrates, CH_4+n-C_4H_{10} and CH_4+iso-C_4H_{10}, showed different trends to that observed in CH_4+C_3H_8 hydrate. It seems that the CH_4+iso-C_4H_{10}, and CH_4+n-C_4H_{10} hydrates have no barrier to dissociation and can be easily broken up, nevertheless, the progress is slow. At the same cavity occupancy of 70.8% for the three sII hydrates, it is evident that within the initial 20–30 ns of the simulation, approximately 12%, 29%, and 25% of the cavities collapsed for CH_4+C_3H_8, CH_4+n-C_4H_{10}, and CH_4+iso-C_4H_{10} hydrates, respectively. This suggests that CH_4+n-C_4H_{10} hydrate may have experienced slightly more and relatively smoother damage compared to the other two, under the assumption of the same cavity occupancy.

In general, the variation of the total hydrate cavity clusters over time in the simple CH_4 hydrate and the mixed CH_4+CO_2 hydrate is pronounced and indicates a dynamic decomposition and reformation of the cages, these variations are already reduced for the CH_4+C_3H_8 hydrate and even less pronounced for the other two sII mixed hydrates.

To gain more details about which type of the cavity is reformed over the dissociation process, Fig. 7 presents a time-dependent overview of this parameter for different systems. During the dissociation, fluctuations could be observed in the number of 5^{12} cavities for simple CH_4 hydrate, as well as mixed CH_4+CO_2 hydrates and CH_4+C_3H_8 hydrate. Only CH_4 and – in the case of the mixed CH_4+CO_2 hydrate – also CO_2

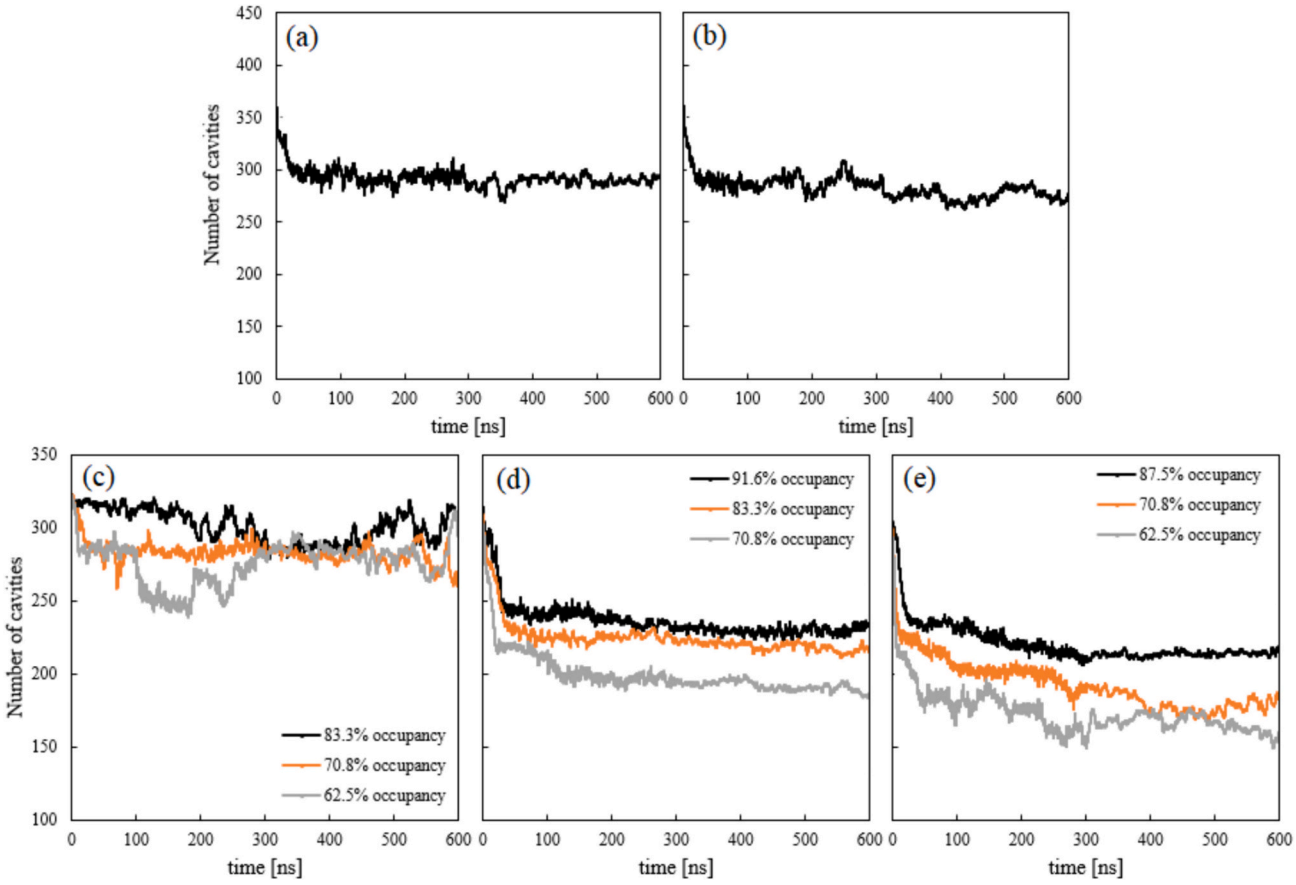

Fig. 6. The smoothed time variation of the total hydrate cavity clusters over the entire simulation of (a) CH_4 hydrate, (b) CH_4+CO_2 hydrate, (c) CH_4+C_3H_8 hydrate, (d) CH_4-n-C_4H_{10}, and (e) CH_4+ iso--C_4H_{10} hydrate. It includes all possible cavity types of each structure. The calculations of sII hydrates with different cavity occupancies are shown here; A differentiated description of the percentage occupancy of the 5^{12} and $5^{12}6^4$ cages of sII hydrates can be found in Table 2.

was involved into this process. In the case of CH_4+iso-C_4H_{10} and CH_4+n-C_4H_{10} hydrate dissociation the number of 5^{12} cavities continuously decreases. With regard to the decrease of the large cages, namely $5^{12}6^2$ for sI hydrates and $5^{12}6^4$ for the hydrates of sII the following developments can be observed: After a short decrease at the beginning, the number of $5^{12}6^2$ cavities belonging to the sI hydrates also showed fluctuations, with CH_4 and CO_2 being involved in the process, respectively. In the dissociation process of the CH_4+C_3H_8 hydrate, fluctuations were observed in the number of $5^{12}6^4$ cavities, however, it maintained at a nearly constant level. For the other two sII hydrates containing n-C_4H_{10} or iso-C_4H_{10}, it continuously decreased over time. So, the main cavity types of 5^{12}, $5^{12}6^2$, and $5^{12}6^4$ cavities could be reformed during the dissociation process of CH_4, CH_4+CO_2, and CH_4+C_3H_8 hydrate, but this reformation was not significantly observed for CH_4+iso-C_4H_{10} and CH_4+n-C_4H_{10} hydrate dissociation. Moreover, the simulations also show that a few new cavity types, namely $4^15^{10}6^2$, $5^{12}6^3$ and $4^15^{10}6^4$, crystalized in the quasi-liquid phase after the breakup of the initial hydrate cavities for all systems. This observation proves the generation of new hydrate cavities after starting the hydrate dissociation and not only the preservation of already existing cavities. It should be noted that these cavities comprise an odd number of water molecules that are transiently stable, not long-lived, and would eventually transition to a more stable cavity [51]. For instance, a $4^15^{10}6^2$ cavity is topologically closely related to the $5^{12}6^2$ cavity, allowing it to easily reconfigure into a proper large $5^{12}6^2$ cavity [52].

In addition, the number of empty cavities (without a gas molecule) was also counted. It is evident that some empty cavities were formed in the case of sI hydrates, as the sI hydrates did not initially involve empty cavity in this simulation. On the other hand, sII hydrates had initially empty cavities, and the number of empty cavities also fluctuated (indicating reforming) during the dissociation of CH_4+C_3H_8 hydrate.

The percentage of gas released. Fig. 8 presents the calculated amount of released gas and the contribution of gas molecules in the gas hydrate dissociation. In sI hydrates dissociation (Fig. 8a), the release of CH_4 molecules fluctuated between 15 and 22%. The released amount of CO_2 exhibited slightly greater fluctuations than that of CH_4, displaying a general constant trend. This suggests that CO_2 is more actively involved in the recrystallization of the cavities than CH_4. Calculations for sII hydrates with varying cavity occupancies were conducted, as illustrated in Figs. 8b-d. During the dissociation of CH_4+C_3H_8 hydrate, the released gas reached a maximum of 20%, displaying pronounced fluctuations in both CH_4 and C_3H_8 release. It can be also found that the rate of C_3H_8 release is obviously lower than that of CH_4. These results indicate that CH_4 and C_3H_8 molecules have the ability to return to the quasi-liquid phase, facilitating the reformation of hydrates. Towards the end of the dissociation process, however, at slight increasing trend in the release of both components can be observed for those CH_4+C_3H_8 hydrates with 70.8% and 83.3% cage occupancy, respectively. This suggests that the self-preservation effect of the C_3H_8 system is only short-lived. In contrast, gas molecules were more readily released in the CH_4+iso-C_4H_{10} and CH_4+n-C_4H_{10} hydrates, as evidenced by the increasing amount of gas released, reaching approximately ~40–50% for these systems (Fig. 8c and d). The release of CH_4, iso-C_4H_{10} and n-C_4H_{10} molecules gradually increased with the breakdown of the hydrate cavities and did not stop. This indicates that the behavior of gas molecules (CH_4) is influenced by the presence of other gases in the mixed gas hydrate. In most systems, the percentage of released CH_4 exceeded that of other components. However, in the last two sII hydrates, this was not

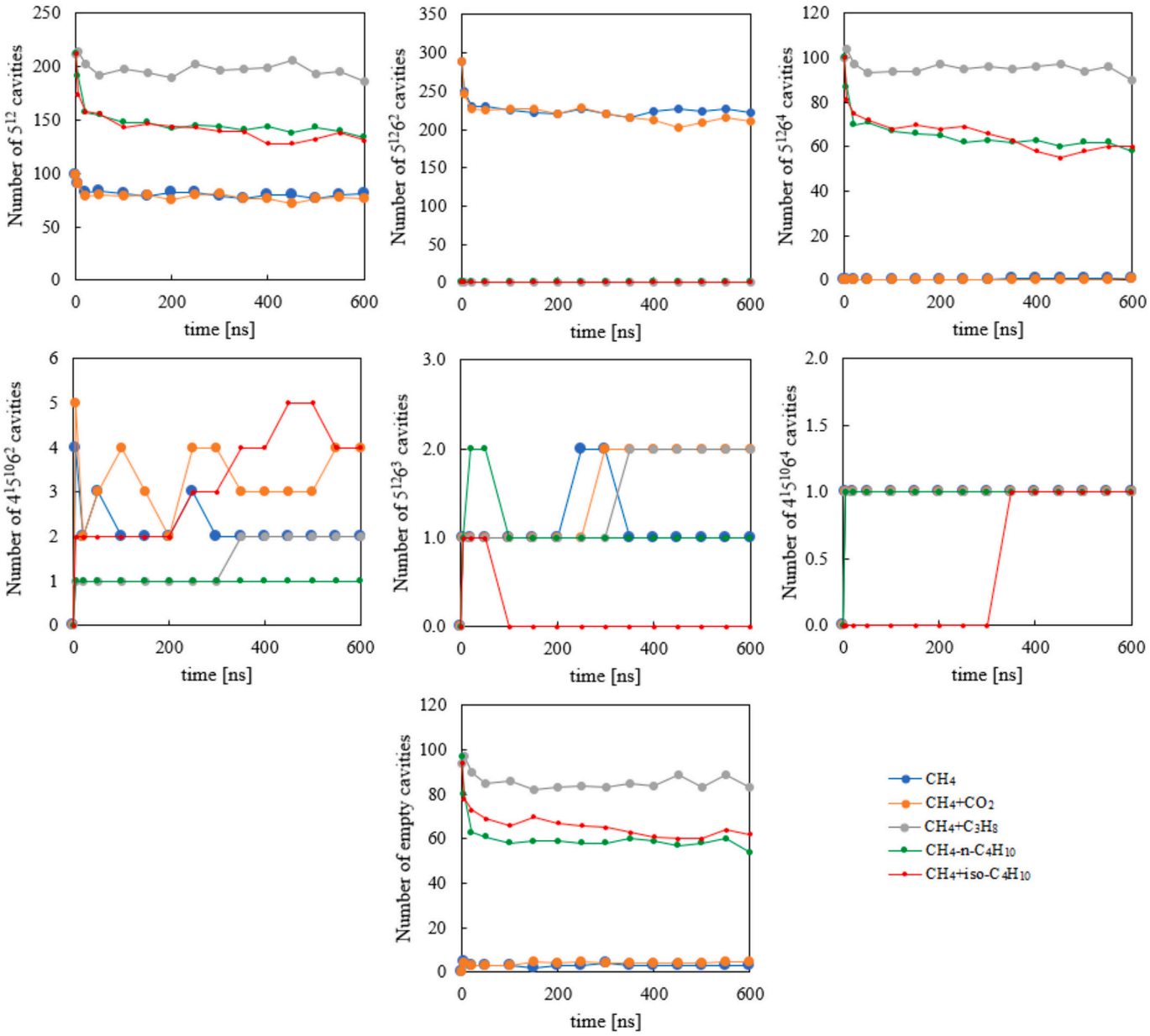

Fig. 7. The time variation of the hydrate cavity clusters over the entire simulation. The hydrate simulation systems are represented by different colors, as indicated in the figure's legend. This figure shows the calculations of sII hydrates with the occupancy of 70.8%.

always the case. In certain mixtures, C_4H_{10} molecules were released more than CH_4.

Furthermore, a decrease in cavity occupancy can facilitate the release of gas molecules due to lower stability in the system.

There is a clear distinction in the dissociation processes of sI and sII hydrates, as evident from both experimental findings and simulations. In general, we can substantiate the reformation or nucleation (in terms of the formation of new cavity types as an intermediate state) of hydrates during the dissociation process. This phenomenon may halt the further dissociation of sI hydrates and, to some extent, sII hydrates, aligning with experimental observations. In particular, gas molecules within sI hydrates effortlessly induce reformation pressure by supersaturating the quasi-liquid phase. Conversely, the contribution of larger hydrocarbons to hydrate reformation appears to be less significant. Each sII hydrate exhibits distinct decomposition behavior, contingent on its composition. Therefore, the gas molecules and their distribution in the sII hydrate particularly are important in the hydrate dissociation process. We should consider that the hydrate composition markedly differs from the initial feed gas, as indicated in Tables 1 and 2. After dissociation, the gas phase composition released from hydrate dissociation closely resembles that within the hydrate phase. For sII hydrates, an evaluation of hydrate reformation potential was conducted using this feed gas composition. The investigation revealed that in the cases of iso-C_4H_{10} and n-C_4H_{10}, the liquefied hydrocarbon phase might be present on the gas/liquid surface due to the significant percentage of these hydrocarbons in which the C_4-hydrocarbons preferentially accumulate. In this case, the self-preservation cannot occur. However, the simulation showed a self-preservation phenomenon for the CH_4+C_3H_8 hydrate, which contrasts with observations in the experiment. The accumulation of C_3H_8 molecules in both the quasi-liquid phase and at the surface results in a temporary stagnation of the hydrate dissociation process. This is not the case in the experiment. As mentioned before, one possible explanation could be that a continuous gas flow was employed in the experiments, ensuring that gas molecules released from the hydrate phase were at least partially removed from the surface. This may generally reduce the accumulation of gas molecules at the gas/liquid interface as well as the

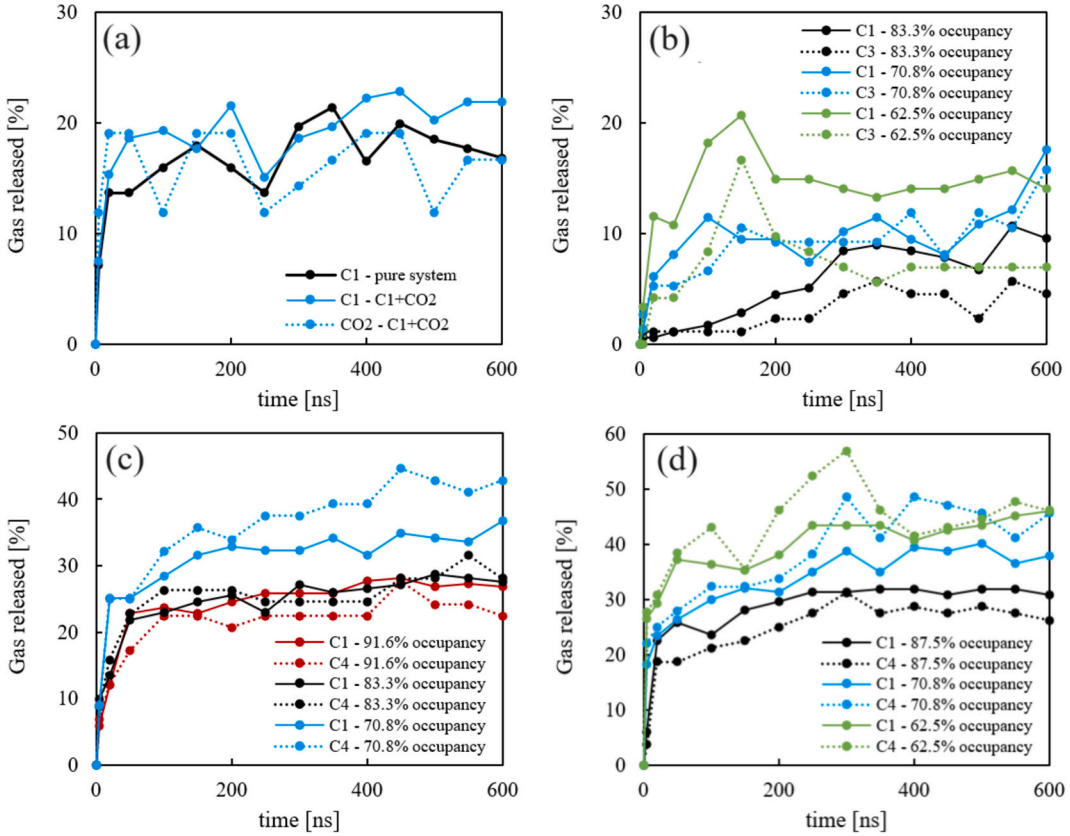

Fig. 8. The time variation of gas released over the entire simulation of (a) CH_4 hydrate and CH_4+CO_2 hydrate, (b) CH_4+C_3H_8 hydrate, (c) CH_4-n-C_4H_{10}, and (d) CH_4+iso-C_4H_{10} hydrate. The calculations of sII hydrates with different cavity occupancies are shown here; A differentiated description of the percentage occupancy of the 5^{12} and $5^{12}6^4$ cages of sII hydrates can be found in Table 2.

liquefaction of heavier hydrocarbons and prevent further interaction with the quasi-liquid phase. However, it could have a greater influence on hydrate reformation for the higher hydrocarbons, as they have a lower tendency to re-migrate into the quasi-liquid phase than CH_4 and CO_2.

4. Summary and conclusions

In this study, an attempt was made to show how different gas molecules can affect the self-preservation effect of gas hydrates. In conclusion, the following outcomes could be extracted for the dissociation behavior of the investigated gas hydrates from the experiments and the MD simulations:

- The experimental data show a self-preservation effect for both the simple CH_4 sI hydrate and the mixed CH_4+CO_2 sI hydrate, whereby the self-preservation effect is more pronounced for the mixed CH_4+CO_2 hydrate than for the simple CH_4 hydrate. For all mixed sII hydrates, however, no self-preservation effect can be observed in the experiments; all show continuous decomposition. However, the rate of decomposition seems to depend on the composition of the hydrates.
- The results of the numerical simulations show that even in the case of hydrate decomposition below the freezing point of water, the water molecules do not directly transform into an ice structure. Instead, they remain disordered as a quasi-liquid layer on the surface of the decomposing hydrate crystal and are incorporated into hydrate reformations.
- For the sI CH_4 hydrate, only the surface of hydrate was dissociated upon the simulation time, but thereafter no further dissociation was observed. CH_4-molecules remain in/revert to the quasi-liquid layer inducing the reformation of hydrate cavities. However, the behavior of CH_4 molecules in the dissociation process is influenced by the presence of other gases in the mixed gas hydrate. For the CH_4+CO_2 hydrate, it was also observed that the surface of hydrate transition into a quasi-liquid layer in which, in addition to the CH_4, large quantities of CO_2 molecules remain most likely due to the good solubility of CO_2. Both types of molecules are therefore available for hydrate reformation. Assuming that in sII hydrates the cavities are not fully occupied with gas molecules, they are expected to decompose faster than the sI hydrates. By decreasing the cavity occupancy, the results show a more pronounced decline in cavities over time, indicating a faster dissociation process. It was observed that the CH_4+iso-C_4H_{10} and CH_4+n-C_4H_{10} hydrates have no barrier to dissociation and can be easily broken up. It is very likely that during the decomposition of these hydrates, a liquid hydrocarbon phase forms under the given conditions, in which the C_4-hydrocarbons preferentially enrich. Thus, the C_4-hydrocarbons are no longer available for hydrate reformation. However, there was no evidence for the formation of a liquid hydrocarbon phase during the decomposition of CH_4+C_3H_8 under the respective conditions. This may explain the slightly different decomposition behavior of the CH_4+C_3H_8 hydrates compared to the C_4-containing hydrates.
- There are still some differences between the MD simulation results and those obtained via the experiments, particularly for the sII hydrates. A possible reason for this could be that a continuous gas flow was used in the experiments, which partially removed the gas released from the hydrate phase. However, the amount of the remaining gas molecules could be sufficient to reform the hydrate. In contrast to the simulations, further interaction especially for the higher hydrocarbons with the quasi-liquid layer was at least reduced in the experiments. Also, the experimentally formed hydrates may

show both partial occupancy of the cavities and defects in their structure, whereby both reduce the stability of hydrate structures compared to an idealized structure in the simulation. Moreover, there are some physical differences between experimental and simulation conditions affecting the dissociation behavior. Last but not least, the simulation results describe a significantly shorter period of time than the experimental data. However, the simulations at the current size provided sufficient information to answer the questions raised by the experiments. A larger simulation cell could yield more precise results, but it would also require significantly more time to achieve meaningful outcomes. Preparing a larger simulation cell can be considered as an extension of this work to evaluate its impact.

Nevertheless, we are convinced, that the results of this study could reveal the dissociation behavior of gas hydrates in nature that may occur at subzero temperatures and pressures higher than 0.1 MPa and also include different gas molecules. The ability of some gas hydrates to delay their decomposition by reformation is of crucial importance in many respects, e.g. for gas storage and transportation and for the response of gas hydrates to climate change. With the results presented in this study, this ability can now possibly be assessed somewhat better.

Supplementary data to this article can be found online at https://doi.org/10.1016/j.apenergy.2024.124042.

CRediT authorship contribution statement

Parisa Naeiji: Writing – original draft, Visualization, Validation, Methodology, Investigation, Conceptualization. **Manja Luzi-Helbing:** Writing – review & editing, Visualization, Validation, Methodology, Investigation, Conceptualization. **Judith M. Schicks:** Writing – review & editing, Supervision, Project administration, Investigation, Conceptualization. **Mengdi Pan:** Writing – review & editing, Investigation.

Declaration of competing interest

The authors declare that they have no known competing financial interests or personal relationships that could have appeared to influence the work reported in this paper.

Acknowledgement: The authors gratefully acknowledge Rudolf Naumann for his invaluable support during the experiments.

Data availability

Data will be made available on request.

References

[1] Sloan ED, Koh CA. Clathrate hydrates of natural gases. 3rd ed. CRC Press; 2008.
[2] Milkov AV. Global estimates of hydrate-bound gas in marine sediments: how much is really out there? Earth Sci Rev 2004;66:183–97.
[3] Paull CK, Dillon WP. Natural gas hydrates: Occurrence, distribution, and detection: Occurrence, distribution, and detection. American Geophysical Union; 2001.
[4] Ruppel CD, Kessler JD. The interaction of climate change and methane hydrates. Rev Geophys 2016;55:126–68.
[5] Chuvilin E, Bukhanov B, Davletshina D, Grebenkin S, Istomin V. Dissociation and self-preservation of gas hydrates in permafrost. Geosciences 2018;8:431.
[6] Bohannon J. Weighing the climate risks of an untapped fossil fuel. Science 2008;319.
[7] Krey V, Canadell JG, Nakicenovic N, Abe Y, Andruleit H, Archer D, et al. Gas hydrates: entrance to a methane age or climate threat? Environ Res Lett 2009;4.
[8] Mascarelli AL. A sleeping giant? Nat Clim Chang 2009;3:46–9.
[9] Tinivella U, Giustiniani M, de la Cruz Vargas Cordero I, Vasilev A. Gas hydrate: environmental and climate impacts. Geosciences 2019;9.
[10] Istomin V, Yakushev V, Makhonina NA, Kwon VG, Chuvilin E. Self-preservation phenomenon of gas hydrates. Digest 2006;4:16–27.
[11] Chuvilin EM, Yakushev VS, Perlova EV. Gas and possible gas hydrates in the permafrost of Bovanenkovo gas field, Yamal Peninsula. West Siberia Polarforschung 2000;68:215–9.
[12] Kuhs WF, Genov G, Staykova DK, Hansen T. Ice perfection and onset of anomalous preservation of gas hydrates. Phys Chem Chem Phys 2004;6:4917–20.
[13] Stern LA, Circone S, Kirby SH, Durham WB. Anomalous preservation of pure methane hydrate at 1 atm. J Phys Chem B 2001;105:1756–62.
[14] Stern LA, Circone S, Kirby SH, Durham WB. Temperature, pressure, and compositional effects on anomalous or "self" preservation of gas hydrates. Can J Phys 2003;81:271–83.
[15] Tse JS, Klug DD. Formation and decomposition mechanisms for clathrate hydrates. J Supramol Chem 2002;2:467–72.
[16] Majid AAA, Koh CA. Intra- and intermolecular interactions between non-covalently bonded species: A volume in. Develop Phys Theor Chem 2021:267–85.
[17] Takeya S, Uchida T, Nagao J, Ohmura R, Shimada W, Kamata Y, et al. Particle size effect of CH4 hydrate for self-preservation. Chem Eng Sci 2005;60:1383–7.
[18] Takeya S, Shimada W, Kamata Y, Ebinuma T, Uchida T, Nagao J, et al. In situ X-ray diffraction measurements of the self-preservation effect of CH4 hydrate. J Phys Chem A 2001;105:9756–9.
[19] Zhong JR, Zeng XY, Zhou FH, Ran QD, Sun CY, Zhong RQ, et al. Self-preservation and structural transition of gas hydrates during dissociation below the ice point: an in situ study using Raman spectroscopy. Sci Rep 2016;6:1–13.
[20] Takeya S, Ripmeester JA. Dissociation behavior of clathrate hydrates to ice and dependence on guest molecules. Angew Chem Int Ed 2008;47:1276–9.
[21] Takeya S, Hachikubo A. Dissociation kinetics of propane–methane and butane–methane hydrates below the melting point of ice. Phys Chem Chem Phys 2021;23:15003.
[22] Belosludov VR, Subbotin OS, Krupskii DS, Ikeshoji T, Belosludov RV, Kawazoe Y, et al. Thermodynamic properties of hydrate phases immersed in ice phase. J Phys Conf Ser 2006;29:198–205.
[23] Gets KV, Zhdanov RK, Bozhko YY, Belosludov VR. Thermodynamic properties of propane and methane hydrates doped with sodium hydroxide. J Phys Conf Ser 2021;2057:012075.
[24] Factorovich MH, Naullage PM, Molinero V. Can clathrates heterogeneously nucleate ice? J Chem Phys 2019;151:114707.
[25] Bai D, Zhang D, Zhang X, Chen G. Origin of self-preservation effect for hydrate decomposition: coupling of mass and heat transfer resistances. Sci Rep 2015;5:14599.
[26] Chuvilin E, Davletshina D. Formation and accumulation of pore methane hydrates in permafrost: experimental modeling. Geosciences 2018;8:467.
[27] Betlem P, Senger K, Hodson A. 3D thermobaric modelling of the gas hydrate stability zone onshore Central Spitsbergen. Arctic Norway Mar Petrol Geol 2019;100:246–62.
[28] Luzi M, Girod M, Naumann R, Schicks JM, Erzinger J. A high-pressure cell for kinetic studies on gas hydrates by powder x-ray diffraction. Rev Sci Instrum 2010;81:125105.
[29] Van Der Spoel D, Lindahl E, Hess B, Groenhof G, Mark AE, Berendsen HJ. Gromacs: fast, flexible, and free. J Comput Chem 2005;26:1701–18.
[30] Takeuchi F, Hiratsuka M, Ohmura R, Alavi S, Sum AK, Yasuoka K. Water proton configurations in structures I, II, and H clathrate hydrate unit cells. J Chem Phys 2013;138:124504.
[31] Abascal JLF, Sanz E, García Fernández R, Vega C. A potential model for the study of ices and amorphous water: TIP4P/ ice. J Chem Phys 2005;122:234511.
[32] Eggimann BL, Sunnarborg AJ, Stern HD, Bliss AP, Ilja Siepmann J. An online parameter and property database for the TraPPE force field. Mol Simul 2014;40:101–5.
[33] Martin MG, Ilja Siepmann J. Transferable potentials for phase equilibria. 1. United-atom description of n-alkanes. J Phys Chem B 1998;102:2569–77.
[34] Hess B, Bekker H, Berendsen HJC, Fraaije JGEM. LINCS: a linear constraint solver for molecular simulations. J Comput Chem 1997;18:1463–72.
[35] Docherty H, Galindo A, Vega C, Sanz E. A potential model for methane in water describing correctly the solubility of the gas and the properties of the methane hydrate. J Chem Phys 2006;125:074510.
[36] Darden T, York D, Pedersen L. Particle mesh Ewald: an N·log(N) method for Ewald sums in large systems. J Chem Phys 1993;98:10089–92.
[37] Alavi S. Molecular simulations: Fundamentals and practice. Weinheim, Germany: Wiley-VCH Verlag GmbH; 2020.
[38] Hoover WG. Canonical dynamics: equilibrium phase-space distributions. Phys Rev A 1985;31:1695.
[39] Parrinello M, Rahman A. Polymorphic transitions in single crystals: a new molecular dynamics method. J Appl Phys 1981;52:7182–90.
[40] Hockney RW, Goel SP, Eastwood J. Quiet high resolution computer models of a plasma. J Comput Phys 1974;14:148–58.
[41] Luzi M, Schicks JM, Naumann R, Erzinger J. Systematic kinetic studies on mixed gas hydrates by Raman spectroscopy and powder X-ray diffraction. J Chem Thermodyn 2012;48:28–35.
[42] Luzi M. Kinetic studies on mixed gas hydrates: University of Potsdam. 2012.
[43] Smith C, Pack D, Barifcani A. Propane, n-butane and i-butane stabilization effects on methane gas hydrates. J Chem Thermodyn 2017;115:293–301.
[44] Kou X, Li XS, Wang Y, Zhang Y, Chen ZY. Distribution and reformation characteristics of gas hydrate during hydrate dissociation by thermal stimulation and depressurization methods. Appl Energy 2020;277:115575.
[45] Yang M, Zhao J, Zheng J, Song Y. Hydrate reformation characteristics in natural gas hydrate dissociation process: a review. Appl Energy 2019;256:113878.
[46] Humphrey W, Dalke A, Schulten K. VMD: Visual molecular dynamics. J Mol Graph 1996;14:33–8.
[47] Naeiji P, Woo TK, Alavi S, Varaminian F, Ohmura R. Interfacial properties of hydrocarbon/water systems predicted by molecular dynamic simulations. J Chem Phys 2019;150:114703.
[48] Davidson DW, Gough SR, Lee F, Ripmeester JA. Revue de Chimie Minérale. Tom 1977;14:447.

[49] Chen Y, Chen C, Sum AK. Propane and water: the cooperativity of unlikely molecules to form clathrate structures. J Phys Chem B 2020;124:4661–71.
[50] Chen Y, Chen C, Sum AK. Molecular resolution into the nucleation and crystal growth of clathrate hydrates formed from methane and propane mixtures. Cryst Growth Des 2021;21:960–73.
[51] Walsh MR, Rainey JD, Lafond PG, Park DH, Beckham GT, Jones MD, et al. The cages, dynamics, and structuring of incipient methane clathrate hydrates. Phys Chem Chem Phys 2011;13:19951–9.
[52] Belosludov RV, Gets KV, Zhdanov RK, Bozhko YY, Belosludov VR, Chen LJ, et al. Molecular dynamics study of clathrate-like ordering of water in supersaturated methane solution at low pressure. Molecules 2023;28:2960.